Effect of Composition and Configuration on Hindered Diffusion of Residue Fractions through Polycarbonate Membranes

Zhentao Chen, Jinsen Gao, Suoqi Zhao, Zhiming Xu, and Chunming Xu
State Key Laboratory of Heavy Oil Processing and College of Chemical Engineering, China University of Petroleum, Changping, Beijing 102249, P.R. China

DOI 10.1002/aic.13884
Published online July 25, 2012 in Wiley Online Library (wileyonlinelibrary.com).

Diffusion behavior of narrow fractions of three residues and subfractions of a residue through four polycarbonate membranes was investigated using a diaphragm cell at 308 K. The results show that the diffusivities of fractions with similar molecular weight behaved differently. Comparisons among SAR subfractions (saturates, aromatics, and resins) of the same fraction show that saturates has the largest diffusion coefficient, followed by aromatics, and then resins. The diffusion coefficients of fractions fall among that of their subfractions. The regular variation of diffusivity along with the properties for fractions with similar molecular weight is an indication of the difference in their diffusivities resulting from the difference in their compositions and structures. Hindrance factors of the subfractions through membranes with small pores have a similar variation trend as their diffusion coefficients. The hindrance factors of the feedstocks in 50 and 80 nm pore size membranes are mostly larger than 0.90, but the values in 15 nm membranes range from 0.55 to 0.81. The study not only indicates that the diffusional limitations are significant in pores with the typical hydrotreating catalyst size but composition and configuration have an effect on the hindered diffusion of residue molecules.. © 2012 American Institute of Chemical Engineers *AIChE J,* 59: 1369–1377, 2013

Keywords: hindered diffusion, diffusion coefficient, membrane, residue, configuration effect

Introduction

Production of clean fuels from petroleum residue is becoming crucial to satisfy the increasing energy demands as conventional oil continually depletes. It is well-known that the catalytic conversion of residue is strongly influenced by diffusion resistance, in part due to the fact that the size of most residue species is comparable to the average pore diameters of typical hydrotreating catalysts. Resistance to diffusion would significantly reduce the effectiveness of the catalysts and the overall catalytic reaction rate. Therefore, the knowledge of diffusion behavior of residue molecules is vital to the design of efficient catalyst and hydroconversion performance of heavy feedstocks.

Hindered diffusion of heavy oil molecules has been studied extensively by diaphragm diffusion cell,[1–3] adsorptive uptake,[4–6] and reactive kinetic methods.[7–9] All experimental results to date confirmed that the hindered effect is significant for residue molecules diffusing through pores with typical hydrotreating catalyst size. More recently, modeling results also revealed that intraparticle diffusion is a crucial factor for residue hydrotreating processes.[9,10] However, the hindered magnitude of diffusion for residue molecules varies across the investigations.[1,4,7,11] Because of the extreme complexity in an actual feedstock, it is difficult to obtain detailed diffusion behavior of petroleum residue without appropriate separations.

In our previous study, Athabasca oil sand bitumen vacuum residue (AVR) was separated by a supercritical fluid extraction and fractionation (SFEF) technique, and hindered diffusivities of five AVR SFEF fractions through polycarbonate membranes were investigated.[12] The results showed that the hindered degree of diffusion for the fractions is higher than the predicted value from the Renkin equation,[13] which derives from a hydrodynamic theory model of noninteracting spherical particles moving along the centerline of the cylindrical pore. A number of theoretical and experimental studies have confirmed that diffusion of nonspherical solutes deviate from the Renkin equation.[14–17] Unfortunately, there has not yet been any detailed publication concerning the effect of configuration on the diffusion behavior of petroleum residue molecules. Therefore, a further study on this aspect is necessary to understand the published results.

The primary focus of the present study is on extending investigation of residue molecule diffusivity through polycarbonate membranes to include the influence of composition and molecular configuration. Three residues were applied as feedstocks in this study. The diffusion coefficients of SFEF fractions of the residues are determined and that of fractions with similar molecular weight are compared. Furthermore, AVR SFEF fractions were subdivided into SAR subfractions (saturates, aromatics, and resins). The effect of molecular configuration was taken into account by comparing diffusion behavior of SAR subfractions.

Hindered Diffusion

It should be noted that the hindrance factor, the ratio of effective to bulk diffusion coefficient of a solute molecule,

Correspondence concerning this article should be addressed to C. Xu at xcm@cup.edu.cn.

has been commonly used to quantitatively describe the hindered degree of diffusion. Most hindered diffusion studies attribute hindrance to two factors: steric restriction and hydrodynamic drag resistance. Both of the factors depend on the ratio of solute size to pore size, $\lambda = d/d_p$. Here, d and d_p are solute size and pore size, respectively.

Numerous theoretical correlations have been proposed to relate hindrance factor to λ. Combining equilibrium partition coefficients from Ferry[18] and centerline drag coefficients from Lane[19] allowed Renkin to obtain the relationship[13]

$$D_e/D_b = F(\lambda) = (1-\lambda)^2(1 - 2.104\lambda + 2.09\lambda^3 - 0.95\lambda^5) \quad (1)$$

where D_e is the effective diffusion coefficient of solute through membrane, D_b is the bulk diffusion coefficient of solute, and $F(\lambda)$ is the hindrance factor of diffusion. The Renkin equation is considered accurate for $\lambda < 0.5$. Good agreement between the Renkin equation and experimental data has been observed.[8,20] However, not all studies support it.[7,21] Therefore, several alternative empirical expressions have been developed. The following power-law relationship is one that has been used in hindered diffusion studies[7,22]

$$F(\lambda) = (1-\lambda)^m \quad (2)$$

The parameter m indicates the hindered magnitude of diffusion. When $m = 4.4$, the power law's predictions approach that of the Renkin equation.

Experimental

Feedstock preparation

Canada AVR, Chinese Dagang vacuum residue (DVR), and Kazakhstan vacuum residue (KVR) were used as feedstocks. Each residue was separated into several fractions and an endcut by the SFEF technique. Subfractions were obtained by a two-step process of SFEF technique followed by SAR separation. The separation process and operating procedure have been reported elsewhere.[23,24] It is known that properties, such as molecular weight, of SFEF fractions vary gradually with increased SFEF yield. Hence, every third fraction (SFEF-3, SFEF-6…) of the residues was chosen as feedstocks for the diffusion experiments. SARA (saturates, aromatics, resins, and asphaltenes) analyses were performed according to the procedures described by Liang.[25] The residues and the corresponding SFEF fractions were subjected to various analyses. The average molecular weight was determined in toluene at 45°C using a Knauer vapor pressure osmometer (Knauer Instruments, Germany). The elemental analysis was carried out on a Perkin-Elmer CHNS/O Analyzer 2400 (Perkin-Elmer).

Toluene was used as solvent for the diffusion experiments. The solution was filtered through a 2 μm pore filter before preparation. A 10 g/L solution of each feedstock in toluene was agitated at room-temperature for 24 h.

Diaphragm diffusion cell

The diffusion experiments were performed using a diaphragm diffusion cell described in detail elsewhere.[12] A brief summary of the diffusion cell is given below. The apparatus illustrated in Figure 1 contains two glass chambers clamped together with a membrane between them. Teflon-coated magnetic stirring bars are mounted in the chambers and are driven by the rotation of an external magnet. To maintain a constant temperature, the cell was placed in a thermostatic bath during experiments.

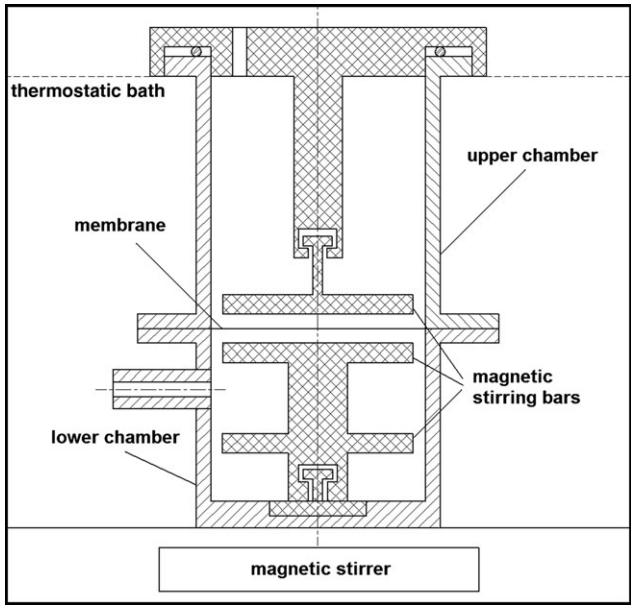

Figure 1. Schematic diagram of diaphragm diffusion cell apparatus.

The lower and upper chamber hold a volume of 48.1 ml and 55.3 ml, respectively, which were measured by weighing the cell before and after filling with deionized water. Track-etched Nuclepore polycarbonate membranes with nominal pore diameters of 15, 50, 80, and 1000 nm (Whatman) were used in the diffusion experiments. The thickness of these membranes measured by scanning electron microscopy photographs is 6.64, 6.66, 6.66, and 11.01 μm, respectively. This type of membranes is extensively used in the study of diffusional transport because of their ideal pore geometry.[16,21,26]

Diffusion coefficient measurements

Diffusion coefficient measurements were performed using the diaphragm diffusion cell mentioned above. The method for measuring diffusion coefficient is described in detail elsewhere.[12] A brief description is given below.

The same procedure for measuring diffusivity was applied in each case. Initially, the lower chamber was filled with solution and the upper chamber with pure solvent. Discrete samples (about 2 ml) were withdrawn from the upper chamber at appropriate time intervals. Then, an equal volume of pure toluene was added to the upper chamber to keep the volume constant. The diffusion experiment ended when equilibrium was approached. The concentrations of the samples and the final solutions in the upper and lower chambers were determined by evaporating the solvent and weighing the residue. The concentration in the lower chamber corresponding to the sampling point was determined from mass balance.

In the pseudo-steady-state, the flux across the membrane in incremental time dt equals the change in the amount of solute in any chamber. So combining mass balance of two chambers and diffusion flux through membrane pores, one obtains

$$\frac{d}{dt}(c_L - c_U) = -\frac{S}{l}\left(\frac{1}{V_L} + \frac{1}{V_U}\right)D(c_L - c_U) \quad (3)$$

Table 1. Properties of the Residues and Their Fractions

Feeds	Molecular Weight	Density (g/cm^3)	H/C (−)	Sulfur (wt %)	Saturates (wt %)	Aromatics (wt %)	Resins (wt %)	Asphaltenes (wt %)
AVR	1147	1.060	1.43	6.05	7.80	41.52	32.60	18.09
AVR-3	643	0.984	1.62	3.99	14.78	68.03	18.16	0
AVR-6	748	1.008	1.54	4.82	5.07	63.32	31.41	0
AVR-9	903	1.039	1.38	5.43	0	61.43	38.13	0
AVR-12	1599	1.067	1.37	6.48	0	48.15	58.72	0
DVR	1008	0.980	1.59	0.24	28.00	34.28	36.01	1.72
DVR-3	776	0.931	1.75	0.21	52.58	32.5	14.92	0
DVR-6	890	0.936	1.75	0.23	45.44	37.09	17.46	0
DVR-15	1759	0.990	1.52	0.30	0.89	38.48	60.63	0
KVR	731	0.935	1.72	2.61	53.95	26.43	16.88	0
KVR-6	735	0.905	1.83	1.90	69.70	22.23	8.10	0
KVR-9	923	0.906	1.78	2.20	66.68	24.60	8.70	0
KVR-18	1557	0.960	1.62	3.91	15.15	51.05	33.80	0

where D is the diffusion coefficient of solute, c_L and c_U refer to solute concentrations in the lower and the upper chamber of the diaphragm cell, V_L and V_U are the volumes of the lower and upper chamber, S is the effective diffusion area of the membrane pores and l is the effective diffusion path length.

Integrating Eq. 3 between the jth and $(j + 1)$th sampling, we have

$$\ln\frac{c_{L,j+1} - c_{U,j+1}}{c_{L,j} - c_{U,j}} = -\beta D_j \Delta t_{j,j+1} (j = 0, 1, 2\ldots\ldots) \quad (4)$$

In this equation, the subscripts j and $j + 1$ refer to the sampling numbers, t is the time of sampling, D_j is the average diffusion coefficient of the solute transporting through the pores between the jth and $(j + 1)$th sampling, and β is the constant of the diaphragm cell and is given by Eq. 5

$$\beta = \frac{S}{l}\left(\frac{1}{V_L} + \frac{1}{V_U}\right) \quad (5)$$

An aqueous solution of potassium chloride at 298 K was used to determine β in this study. The method is described elsewhere[27–29] and the diaphragm cell constants with the four membranes are provided in our previous study.[12]

The mass balances were checked for each of the diffusion experiments. The results show that the mass of the solute in the lower chamber at the beginning of the experiment equaled the mass of the solute in both chambers at the end of the experiment. The differences in the mass measurements are less than 0.6%. Furthermore, the error in the diffusion coefficient measurement was analyzed. The results indicate that it is mainly caused by the experimental errors in concentrations and diaphragm cell constant measurements. The largest values of them are 3.12 and 0.29%, respectively, for the chosen AVR fractions.

Results and Discussion

Properties of the residues and the SFEF fractions

The main properties of three residues and their SFEF fractions used in this work are summarized in Table 1. The properties of the residues vary over a wide range. In comparison, AVR has the lowest H/C atomic ratio and largest sulfur content, KVR has the largest H/C atomic ratio, and DVR has the lowest sulfur content. AVR is highly aromatic and has large aromatic and resin components. KVR is relatively paraffinic and has the largest amount of saturates. The properties of DVR fall between that of AVR and KVR.

There is large variation in the properties of the SFEF fractions within a given residue. Molecular weight increases as the fractions become heavier. Density has the similar variation trend as molecular weight, whereas H/C atomic ratio has the opposite variation trend. Saturates are concentrated in the light SFEF fractions, whereas aromatic and resin components are enriched in the heavy fractions.

Effect of composition on diffusion

The results of our previous study showed that the diffusion coefficients of AVR fractions through four membranes are time-dependent.[12] To illustrate this, the diffusion coefficients of three fractions among three residues through 15-nm pore size membranes are plotted against experimental time in Figure 2.

The results show that the diffusion coefficients of each fraction decrease gradually as the experiment proceeds. It is well-known that residue molecules, especially asphaltenes, have significant adsorption on metallic and mineral surface.[30,31] As a result, repeated diffusion of the same feedstock solution was used to test residue adsorption in membrane pores. Of continuously duplicate runs, the results were quite reproducible. As a result, residue molecules are not significantly absorbed in the pores of the polycarbonate membranes and the influence of physisorption on diffusion is excluded from consideration. Therefore, time-dependent

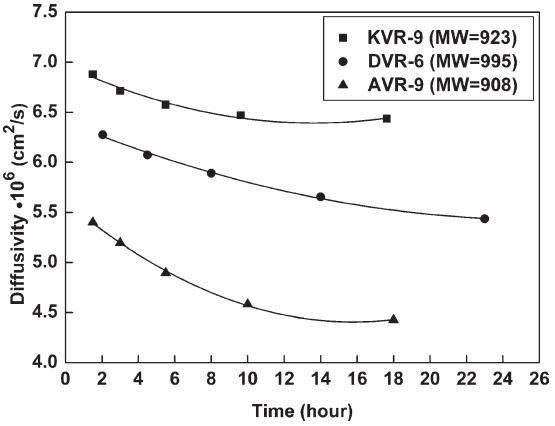

Figure 2. Effective diffusion coefficients of three fractions with similar molecular weight in 15-nm pore size membranes.

Table 2. Comparison of Average Diffusion Coefficients of SFEF Fractions for Three Residues

Fraction	Molecular Weight	$\overline{D} \times 10^6$ (cm^2/s) 15 (nm)	50 (nm)	80 (nm)	1000 (nm)	$\overline{D_b} \times 10^6$ (cm^2/s)
KVR-6	735	6.82	7.93	8.25	8.70	8.64
DVR-3	776	6.10	7.22	7.30	7.85	7.78
AVR-6	748	5.82	7.13	7.41	7.56	7.70
KVR-9	923	6.55	7.73	8.15	8.64	8.56
DVR-6	995	5.72	6.53	6.89	7.03	7.07
AVR-9	908	4.66	6.05	6.48	6.63	6.78
KVR-18	1557	3.67	4.98	5.33	5.62	5.71
DVR-15	1312	3.75	5.22	5.32	5.74	5.83
AVR-12	1599	2.95	4.62	5.03	5.17	5.43

diffusion coefficients illustrate that these fractions are polydisperse mixtures and contain a large number of substances with a range of molecular sizes. The smaller species diffuse more readily through the membrane pores, resulting in decreasing diffusion coefficients as the experiment progresses.

In comparison, it is revealed from Figure 2 that DVR-6 exhibits lower diffusivity than KVR-9 and higher diffusivity than AVR-9. As can be seen from Table 1, these three fractions have similar molecular weights. The results of our previous study showed that the diffusion coefficients decrease as AVR fractions become heavier.[12] To examine the diffusion behavior of residue molecules further, an average diffusion coefficient for a SFEF fraction has been defined and calculated from the diffusion coefficients distribution by Eq. 6.

$$\overline{D_{e_i}} = \frac{\sum_{j=1}^{n} (D_{i,j} \times m_{i,j})}{\sum_{j=1}^{n} m_{i,j}} (i = 3, 6, 9...; j = 1, 2...n) \quad (6)$$

where $\overline{D_{e_i}}$ is the average diffusion coefficient of the ith fraction and $m_{i,j}$ is the amount of the ith fraction through the membrane in the jth interval. The calculated average effective and bulk-phase diffusion coefficients of the fractions of three residues are summarized in Table 2. Here, the bulk-phase diffusion coefficients were determined by extrapolating the effective diffusion coefficients through the four membranes to infinite pore diameter. The detail was described elsewhere.[12]

Table 2 presents that the mean bulk-phase diffusion coefficients of fractions range from 5.43×10^{-6} cm^2/s to 8.64×10^{-6} cm^2/s. In recent years, there have been several studies on the measurement of asphaltene bulk-phase diffusivity in toluene. Durand et al.[32] found the infinite diffusion coefficient for Buzurgan asphaltenes to be about 2.4×10^{-6} cm^2/s by means of ^{1}H diffusion-ordered spectroscopy NMR. Lisitza et al.[33] observed that the diffusion coefficient of UG8 asphaltenes was 2.9×10^{-6} cm^2/s below 0.3 g/L concentration. Fluorescence correlation spectroscopy showed that the translational diffusion coefficients of several petroleum asphaltenes are about 3.5×10^{-6} cm^2/s.[34,35]

The bulk-phase diffusion coefficients of the SFEF fractions in this study are larger than that of asphaltenes mentioned in the above literature. Different diffusion coefficients among four fractions and asphaltenes for heavy crude oil have previously been determined by Durand et al.[36] The diffusion coefficient of the residue fraction is more than three times as large as that of asphaltenes in their study. Thus, the results of the current work can be reasoned due to the distinct compositions and properties between fractions and asphaltenes.

As shown in Table 2, there are significant differences in average diffusion coefficients of fractions across the three residues in each group, which includes the fractions with similar average molecular weight. For diffusing through the same size membranes, KVR fractions with similar molecular weight have the largest average diffusion coefficient, followed by DVR, and then AVR. Furthermore, average diffusion coefficient of KVR-18 is similar to that of DVR-15, although the molecular weight of the former is much larger than that of the latter. Obviously, the diffusivity of residue molecules with similar molecular weight presents a regular variety. Therefore, the pore size appropriate for residue diffusion has to take the composition of the particular feeds into consideration.

With an attempt to interpret the distinction of diffusion behavior for the fractions of different residues, the detailed property analyses of them are described here. The analytical data in Table 1 show that there is a positive variation trend in properties of the fractions with similar molecular weights. The AVR fraction has the largest density and lowest H/C atomic ratio. For the KVR fraction, the situation is reversed. The properties of the DVR fraction fall between that of the AVR and KVR fractions. A characterization index, which is a function of H/C atomic ratio, molecular weight, and density, has been proposed and can be correlated well with many properties of residues and their fractions.[37] Therefore, variation of the diffusion coefficients of the fractions with similar molecular weight as H/C atomic ratio and density seems reasonable. It indicates that the composition of the fractions has an effect on their diffusivity. In this regard, the textural of the catalyst must be matched with the properties of the feeds.

Table 1 also shows that the AVR fraction has the largest aromatic and resin contents while having the smallest saturate contents. The SAR composition of the KVR fraction is opposite as that of the AVR fraction. The DVR fraction has relatively even composition compared with fractions of the other two residues. In a recent study, the significant differences in the average structure of the SAR subfractions of the same SFEF fraction have been presented by Zhang et al.[38] The condensation degree of saturates is smaller than that of aromatics, which are in turn smaller than that of resins. A large research effort has been devoted to studying the configuration effect on diffusivity of macromolecules.[16,17,21,39] Most of the results showed that bulk-phase and hindered diffusivities of macromolecules with different molecular configurations behaved more or less differently. Combining the study of Zhang et al.[38] with that of configuration effect on diffusion of macromolecules,[16,17,21,39] one can predict the different diffusion behavior of SAR components in a fraction. Based on the prediction, the distinction of diffusion behavior for fractions with similar molecular weight for different residues was deducted to be caused by different SAR composition among them.

As mentioned above, hindered diffusion of heavy oil molecules has been investigated extensively via three methods. There are some differences of hindered degree among these studies,[1,4,7,11] which might partly due to different feedstock compositions. A wide range of heavy feeds available for

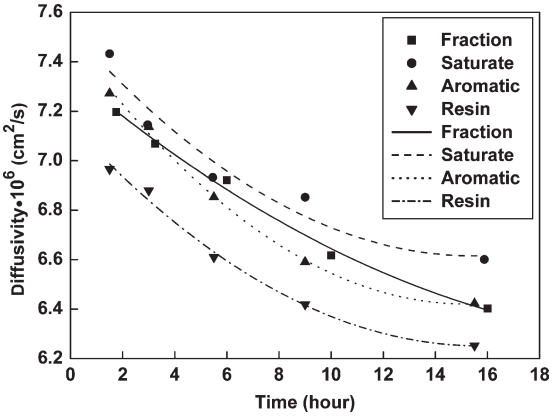

Figure 3. Effective diffusion coefficients of AVR-3 and its subfractions in 15-nm pore size membranes.

refineries suggests the need for designing tailor-made catalysts suitable for a particular feed. Stimulated by this reason, a further study on the diffusion behavior of heavy feedstocks needs to be performed.

Effect of configuration on diffusion

To gain some insight into the diffusional discrepancy of fractions with similar molecular weight, the runs of diffusion experiments of four SFEF fractions of AVR and their subfractions were carried out under the same conditions. The effective diffusion coefficients of AVR-3 and its subfractions through 15-nm pore size membranes are plotted against the experimental time in Figure 3.

As shown in Figure 3, the effective diffusion coefficients of AVR-3 and its subfractions decrease gradually as the experiment proceeds, which is similar to the trend in Figure 2. Comparison of the data shows that the diffusion coefficients differ among three SAR subfractions of AVR-3. The diffusivities rank as follows: saturates has the largest effective diffusion coefficient, followed by aromatics and finally resins. Average diffusion coefficients of four chosen AVR fractions and their subfractions through four membranes are summarized in Tables A1–A4 of the Appendix. Tables A2–A4 show that diffusion behavior of the other three fractions and their subfractions is similar to that of AVR-3 in Figure 3. The results validate the prediction proposed above: diffusivities of SAR subfractions over a given fraction are different.

The data in the Appendix show that the diffusion coefficients of fractions fall among the values of their subfractions. A fraction is comprised of various SAR components. Accordingly, a model correlating diffusion coefficient of a fraction with that of its subfractions is proposed and expressed as

$$\overline{D_F} = ew_S\overline{D_S} + fw_A\overline{D_A} + gw_R\overline{D_R} \tag{7}$$

where $\overline{D_F}$ is the average diffusion coefficient of a fraction, $\overline{D_S}$, $\overline{D_A}$, and $\overline{D_R}$ refer to the average diffusion coefficients of its saturate, aromatic, and resin subfractions through the same pore size membranes, respectively, w_S, w_A, and w_R are the corresponding weight percentage of the subfractions in the fraction, and e, f, and g are correlation coefficients. The experimental average diffusion coefficients of AVR fractions and their subfractions are plotted vs. average molecular weight in Figure 4. The corresponding values and the average diffusion coefficients of fractions determined from Eq. 7 are summarized in Table 3.

Figure 4 shows that the average diffusion coefficients of fractions and their subfractions decrease as fractions become heavier and membrane pores become narrower. Results have shown that bulk-phase diffusivity values of vacuum residue fractions follow a power law relationship with molecular weight.[40] Further studies indicate that diffusivity of residue molecules depend on molecular size and pore size.[7,11] Discussion on diffusion hindrance of residue molecules is presented in the following section in more detail. Furthermore, Figure 4 illustrates that the decreasing order among the other three groups of subfractions is consistent with that of AVR-3. Relative to aromatics and resins, saturates have higher diffusivity. Aromatics exhibited higher diffusivity than resins.

From Table 3, it reveals that the predicted diffusion coefficients of fractions are in reasonable agreement with

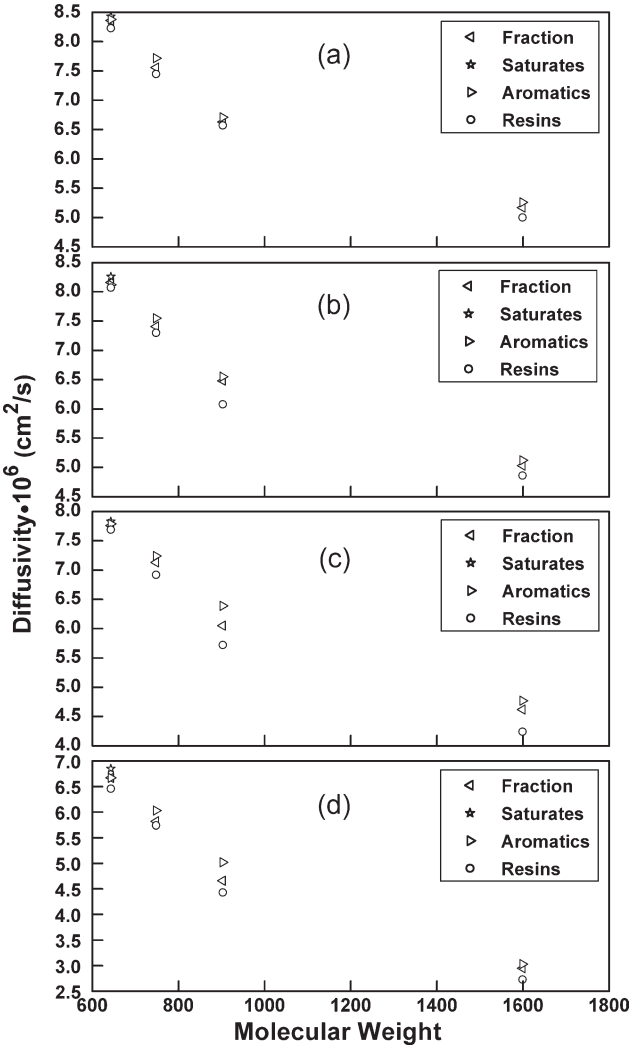

Figure 4. Experimental average diffusion coefficients of AVR fractions and their subfractions vs. average molecular weight for the membranes: (a) 1000 nm, (b) 80 nm, (c) 50 nm, and (d) 15 nm.

Table 3. Experimental Diffusion Coefficients of AVR Fractions and Predicted Values by Their Subfractions

Fraction	d_p (nm)	(10^{-6} cm^2/s) $\overline{D_S}$	$\overline{D_A}$	$\overline{D_R}$	$\overline{D_{F,exp}}$	$\overline{D_{F,pre}}$	Relative Deviation (%)	Constant
AVR-3	15	6.85	6.67	6.46	6.67	6.61	0.96	$e = 2.58, f = 0.40, g = 2.00$
	50	7.83	7.79	7.69	7.76	7.76	0.06	
	80	8.26	8.12	8.07	8.16	8.11	0.66	
	1000	8.43	8.38	8.23	8.36	8.34	0.32	
AVR-6	15	nes	6.03	5.74	5.82	5.87	0.98	$f = 0.74, g = 1.52$
	50	nes	7.24	6.92	7.13	7.06	0.89	
	80	nes	7.55	7.30	7.41	7.41	0.03	
	1000	nes	7.72	7.45	7.56	7.57	0.18	
AVR-9	15	nes	5.02	4.43	4.66	4.73	1.47	$f = 0.71, g = 1.49$
	50	nes	6.39	5.72	6.05	6.07	0.36	
	80	nes	6.55	6.08	6.48	6.35	2.01	
	1000	nes	6.71	6.57	6.63	6.68	0.84	
AVR-12	15	nes	3.03	2.73	2.95	2.94	0.09	$f = 1.60, g = 0.42$
	50	nes	4.77	4.24	4.62	4.62	0.03	
	80	nes	5.12	4.86	5.03	5.03	0.02	
	1000	nes	5.26	5.00	5.17	5.16	0.01	

nes: not enough sample for diffusion experiment.

experimental results. The relative deviations are mostly less than 2%. This indicates that the interaction between residue molecules is negligible due to the fact that the solution is dilute. On the other hand, the diffusion of a fraction is contributed by all its components together. Table 3 also shows that the discrepancies of average diffusion coefficients of subfractions of the same fraction are not distinct. This might result from the slight differences of configuration of subfractions within the same fraction, which has been illustrated in the study of Zhang et al.[38]

A comparison of the correlation coefficients of Eq. 7 between different fractions is provided in Table 3, illustrating that the coefficients are relatively random. Petroleum residue is known to be a very complex mixture, which contains a great variety of compounds and structures. There is not a regular variation in the composition as fractions become heavier. Therefore, a universal model with fixed correlation coefficients cannot be developed. However, a qualitative conclusion can be made from the above comparison. Generally, saturate components diffuse more readily than aromatics and resins with the similar molecular weight. Therefore, it needs to provide more large size pores in catalyst for dealing with aromatic residue than paraffinic residue. As a result, different pore structures of catalyst are required to match various feedstocks even though the average molecular weights of them are similar.

Hindrance factors

As previously mentioned, hindrance factor is the ratio of effective to bulk-phase diffusion coefficients. Therefore, the hindrance factors of AVR fractions and their subfractions diffusing through three membranes with small pore size (15, 50, and 80 nm) are determined accordingly and summarized in Table 4.

As listed in Table 4, hindrance factors decrease as fractions become heavier and membrane pores become narrower. A reduction of 20–43% in diffusion coefficients of fractions occurs at the pore size of 15 nm, which indicates that the intraparticle diffusion resistance is significant for residue molecules through pores with size around typical residue hydrotreating catalysts. The mass transfer limitation of residue molecules is alleviated as the membrane pore size increases to 50 nm. Therefore, it implies that the accessibility of the active sites will be improved when larger pore size are introduced into typical residue hydrotreating catalysts.

Generally, the variation trend of hindrance factor for the subfractions within a given fraction is consistent with the trend in their diffusion coefficients. Resins encounter the strongest resistance in the membrane with the same pore size, followed by aromatics and then saturates. Diffusion of star-branched polymers has been proved to be hindered more intensively than linear polymers.[16] Bohrer et al.[39] also found hindrance factors for branched macromolecules are significantly greater than that for crosslinked macromolecules. Moreover, Zhang et al.[38] found that the average structures of the subfractions within the same SFEF fraction of heavy oil are different. The aromatic ring magnitude and condensation degree of saturates is smaller than that of aromatics and both are smaller than that of resins. Both aromatic ring magnitude and condensation degree of SAR components vary in reverse of effective diffusivity determined in this current study. Therefore, the configuration has an effect on the hindered diffusion of residue molecules. The difference of hindered degree for subfractions of the given fraction results from their different configurations.

Table 4. Hindrance Factors of AVR Fractions and Their Subfractions

Fraction	d_p (nm)	$F(\lambda)$ Fraction	Saturates	Aromatics	Resins
AVR-3	15	0.80	0.81	0.80	0.79
	50	0.93	0.93	0.93	0.93
	80	0.98	0.98	0.97	0.98
AVR-6	15	0.77	nes	0.77	0.77
	50	0.94	nes	0.94	0.93
	80	0.98	nes	0.98	0.98
AVR-9	15	0.70	nes	0.75	0.67
	50	0.91	nes	0.95	0.87
	80	0.98	nes	0.98	0.96
AVR-12	15	0.57	nes	0.58	0.55
	50	0.89	nes	0.91	0.85
	80	0.97	nes	0.97	0.97

nes: not enough sample for diffusion experiment.

Residues have many different compounds with different chemical reactivities and diffusivities. Song et al.[41] showed that the dependence of conversion of two asphaltenes on the catalyst pore size is different because of their different molecular size and configuration. In view of different diffusion resistance of various residue molecules, a commercial catalyst with specific pore structure needs to be designed to achieve high performance. In this regard, tailor-made catalysts with special chemical composition and physical properties are required to match actual residue feedstocks.

Conclusions

In the current study, diffusivities of SFEF fractions of three residues and subfractions of AVR through four porous membranes were investigated quantitatively with a diaphragm cell. The results show that the average bulk-phase diffusion coefficients of SFEF fractions range from 5.43×10^{-6} cm^2/s to 8.64×10^{-6} cm^2/s, which are larger than that of asphaltenes reported in the literature. It can be reasoned due to the distinct compositions between the fractions of this study and asphaltenes in the literature. Furthermore, diffusivities of fractions with similar molecular weight differ with each other for three residues. The variation trend of diffusion coefficients for fractions with similar molecular weight is consistent with that of their properties, such as H/C atomic ratio, density, and SAR composition. Combining distinction of configurations of SAR subfractions with previous studies of configuration effect on diffusivity of macromolecules, different diffusion behavior of the SAR components in a fraction is predicted. The diffusivities of AVR fractions and their subfractions validate this prediction. It indicates that the distinction of diffusion coefficients for fractions of different residues results from different SAR composition among them. Both diffusion coefficients and hindrance factors for AVR subfractions rank as follows: saturates have the largest value, followed by aromatics, and then resins. The comparison among the subfractions validate that composition and configuration have an effect on the diffusion behavior of residue molecules.

Acknowledgments

The authors acknowledge the supports by the China Postdoctoral Science Foundation (No. 2011M500491), the National Natural Science Foundation of China (NSFC) for Young Scholars (No. 21106183), the National Key Basic Research Development Program of China (973 Program) (No. 2010CB226901, 2010CB226902 and 2012CB215001), the Union Fund of China NSFC and CNPC (No. U1162204) and NSFC fund (No. 21176254).

Notation

c = concentration of solution
d = diameter of solute
d_p = diameter of pore
D = diffusion coefficient of solute
$\overline{D}$ = average diffusion coefficient of solute
e, f, g = correlation coefficients
F = hindered factor of diffusion
l = effective diffusion path length
m = the amount of the solute
S = effective diffusion area of the membrane pores
t = time of sampling
V = volume of chamber of diaphragm cell
w = weight percentage of subfractions

Greek letters

β = constant of the diaphragm cell
λ = ration of molecule diameter to pore diameter, d/d_p

Subscript

A = Aromatics
b = bulk diffusion
e = effective diffusion
exp = experimental value
i = the ith SFEF fraction of AVR
j = sampling number
L = lower chamber
pre = predicted value
R = resins
S = saturates
U = upper chamber

Literature Cited

1. Baltus RE, Anderson JL. Hindered diffusion of asphaltenes through microporous membranes. *Chem Eng Sci*. 1983;38:1959–1969.
2. Sane RC, Tsotsis TT, Webster IA, Ravi-Kumar VS. Studies of asphaltene diffusion and structure and their implications for resid upgrading. *Chem Eng Sci*. 1992;47:2683–2688.
3. Dechaine GP, Gray MR. Membrane diffusion measurements do not detect exchange between asphaltene aggregates and solution phase. *Energy Fuels*. 2010;25:509–523.
4. Chantong A, Massoth FE. Restrictive diffusion in aluminas. *AIChE J*. 1983;29:725–731.
5. Yang X, Guin JA. Diffusion-controlled adsorptive uptake of coal and petroleum asphaltenes in a $NiMo/Al_2O_3$ Hydrotreating catalyst. *Chem Eng Commun*. 1998;166:57–79.
6. Tayakout M, Ferreira C, Espinat D, Arribas Picon S, Sorbier L, Guillaume D, Guibard I. Diffusion of asphaltene molecules through the pore structure of hydroconversion catalysts. *Chem Eng Sci*. 2010;65:1571–1583.
7. Tsai M-C, Chen Y-W, Li C. Restrictive diffusion under hydrotreating reactions of heavy residue oils in a trickle bed reactor. *Ind Eng Chem Res*. 1993;32:1603–1609.
8. Lee SY, Seader JD, Tsai CH, Massoth FE. Solvent and temperature effects on restrictive diffusion under reaction conditions. *Ind Eng Chem Res*. 1991;30:607–613.
9. Ferreira C, Marques J, Tayakout M, Guibard I, Lemos F, Toulhoat H, Ramôa Ribeiro F. Modeling residue hydrotreating. *Chem Eng Sci*. 2010;65:322–329.
10. Verstraete JJ, Le Lannic K, Guibard I. Modeling fixed-bed residue hydrotreating processes. *Chem Eng Sci*. 2007;62:5402–5408.
11. Li C, Chen Y-W, Tsai M-C. Highly restrictive diffusion under hydrotreating reactions of heavy residue oils. *Ind Eng Chem Res*. 1995;34:898–905.
12. Chen Z, Xu C, Gao J, Zhao S, Xu Z. Hindered diffusion of residue narrow cuts through polycarbonate membranes. *AIChE J*. 2010;56:2030–2038.
13. Renkin EM. Capillary and cellular permeability to some compounds related to antipyrine. *Am J Physiol*. 1953;173:125–130.
14. Deen WM. Hindered transport of large molecules in liquid-filled pores. *AIChE J*. 1987;33:1409–1425.
15. Davidson MG, Deen WM. Hydrodynamic theory for the hindered transport of flexible macromolecules in porous membranes. *J Membr Sci*. 1988;35:167–192.
16. Bohrer MP, Fetters LJ, Grizzuti N, Pearson DS, Tirrell MV. Restricted diffusion of linear and star-branched polyisoprenes in porous membranes. *Macromolecules*. 1987;20:1827–1833.
17. Deen WM, Bohrer MP, Epstein NB. Effects of molecular size and configuration on diffusion in microporous membranes. *AIChE J*. 1981;27:952–959.
18. Ferry JD. Ultrafilter membranes and ultrafiltration. *Chem Rev*. 1936;18:373–455.
19. Lane JA.*Solvent and extraction and dialysis: dialysis*. In: Perry JH, editor. *Chemical Engineer's Handbook*, 3rd ed.New York:McGraw-Hill Book Company, Inc., 1950:754.
20. Kathawalla IA, Anderson JL. Pore size effects on diffusion of polystyrene in dilute solution. *Ind Eng Chem Res*. 1988;27:866–871.

21. Shao J, Baltus RE. Hindered diffusion of dextran and polyethylene glycol in porous membranes. *AIChE J*. 2000;46:1149–1156.
22. Lee SY, Seader JD, Tsai CH, Massoth FE. Restrictive diffusion under catalytic hydroprocessing conditions. *Ind Eng Chem Res*. 1991;30:29–38.
23. Zhao S, Xu Z, Xu C, Chung KH, Wang R. Systematic characterization of petroleum residua based on SFEF. *Fuel*. 2005;84:635–645.
24. Shi TP, Hu YX, Xu ZM, Su T, Wang RA. Characterizing petroleum vacuum residue by supercritical fluid extraction and fractionation. *Ind Eng Chem Res*. 1997;36:3988–3992.
25. Liang W.*Petroleum Chemistry*, 2nd ed.Dongying:Petroleum University Press, 1995.
26. Macpherson JV, Jones CE, Barker AL, Unwin PR. Electrochemical imaging of diffusion through single nanoscale pores. *Anal Chem*. 2002;74:1841–1848.
27. Woolf LA, Tilley JF. Revised values of integral diffusion coefficients of potassium chloride solutions for the calibration of diaphragm cells. *J Phys Chem*. 1967;71:1962–1963.
28. Wu Y, Ma P, Liu Y, Li S. Diffusion coefficients of L-proline, L-threonine and L-arginine in aqueous solutions at 25 °C. *Fluid Phase Equilibria*. 2001;186:27–38.
29. Smith MJ, Flowers TH, Cowling MJ, Duncan HJ. Method for the measurement of the diffusion coefficient of benzalkonium chloride. *Water Res*. 2002;36:1423–1428.
30. Nassar NN, Hassan A, Pereira-Almao P. Metal oxide nanoparticles for asphaltene adsorption and oxidation. *Energy Fuels*. 2011;25:1017–1023.
31. Saraji S, Goual L, Piri M. Adsorption of asphaltenes in porous media under flow conditions. *Energy Fuels*. 2010;24:6009–6017.
32. Durand E, Clemancey M, Lancelin J-M, Verstraete J, Espinat D, Quoineaud A-A. Aggregation states of asphaltenes: evidence of two chemical behaviors by 1H diffusion-ordered spectroscopy nuclear magnetic resonance. *J Phys Chem C*. 2009;113:16266–16276.
33. Lisitza NV, Freed DE, Sen PN, Song Y-Q. Study of asphaltene nanoaggregation by nuclear magnetic resonance (NMR). *Energy Fuels*. 2009;23:1189–1193.
34. Andrews AB, Guerra RE, Mullins OC, Sen PN. Diffusivity of asphaltene molecules by fluorescence correlation spectroscopy. *J Phys Chem A*. 2006;110:8093–8097.
35. Schneider MH, Andrews AB, Mitra-Kirtley S, Mullins OC. Asphaltene molecular size by fluorescence correlation spectroscopy. *Energy Fuels*. 2007;21:2875–2882.
36. Durand E, Clemancey M, Quoineaud A-A, Verstraete J, Espinat D, Lancelin J-M. ^{1}H diffusion-ordered spectroscopy (DOSY) nuclear magnetic resonance (NMR) as a powerful tool for the analysis of hydrocarbon mixtures and asphaltenes. *Energy Fuels*. 2008;22:2604–2610.
37. Shi T-P, Xu Z-M, Cheng M, Hu Y-X, Wang R-A. Characterization index for vacuum residua and their subfractions. *Energy Fuels*. 1999;13:871–876.
38. Zhang ZG, Guo S, Zhao S, Yan G, Song L, Chen L. Alkyl side chains connected to aromatic units in dagang vacuum residue and its supercritical fluid extraction and fractions (SFEFs). *Energy Fuels*. 2009;23:374–385.
39. Bohrer MP, Patterson GD, Carroll PJ. Hindered diffusion of dextran and ficoll in microporous membranes. *Macromolecules*. 1984;17:1170–1173.
40. Nortz RL, Baltus RE, Rahimi P. Determination of the macroscopic structure of heavy oils by measuring hydrodynamic properties. *Ind Eng Chem Res*. 1990;29:1968–1976.
41. Song C, Nihonmatsu T, Nomura M. Effect of pore structure of nickel-molybdenum/alumina catalysts in hydrocracking of coal-derived and oil sand derived asphaltenes. *Ind Eng Chem Res*. 1991;30:1726–1734.

Appendix

Table A1. Diffusion Coefficients of AVR-3 and Its Subfractions

		$\overline{D} \times 10^6$ (cm^2/s)			
	t (h)	Fraction	Saturates	Aromatics	Resins
15 nm	1.75	7.20	7.43	7.27	6.97
	3.25	7.07	7.15	7.14	6.88
	6	6.92	6.93	6.85	6.61
	10	6.62	6.85	6.60	6.42
	16	6.40	6.60	6.42	6.25
50 nm	0.38	8.09	8.14	8.10	8.05
	0.67	8.00	8.02	7.94	7.95
	1.08	7.89	7.87	7.89	7.90
	1.67	7.74	7.73	7.73	7.69
	2.5	7.60	7.70	7.65	7.50
80 nm	0.38	8.47	8.57	8.47	8.44
	0.67	8.36	8.23	8.28	8.24
	1.08	8.25	8.25	8.22	8.19
	1.67	8.13	8.19	8.14	7.96
	2.5	8.00	8.15	7.94	7.89
1000 nm	0.38	8.91	8.93	8.91	8.75
	0.67	8.57	8.73	8.73	8.60
	1.08	8.31	8.57	8.52	8.37
	1.67	8.25	8.45	8.22	8.13
	2.5	8.16	8.17	8.13	7.99

Table A2. Diffusion Coefficients of AVR-6 and Its Subfractions

		$\overline{D} \times 10^6$ (cm^2/s)			
	t (h)	Fraction	Saturates	Aromatics	Resins
15 nm	1. 5	6.38	nes	6.74	6.37
	3	6.22	nes	6.61	6.20
	5.5	5.96	nes	6.44	6.08
	9.5	5.80	nes	6.16	5.71
	16.5	5.62	nes	5.75	5.52
50 nm	0.38	7.52	nes	7.88	7.67
	0.67	7.39	nes	7.53	7.34
	1.08	7.19	nes	7.27	7.17
	1.67	7.09	nes	7.25	6.61
	2.5	6.97	nes	6.91	6.50
80 nm	0.38	7.90	nes	7.93	7.86
	0.67	7.64	nes	7.78	7.68
	1.08	7.47	nes	7.69	7.39
	1.67	7.30	nes	7.51	7.26
	2.5	7.21	nes	7.37	7.13
1000 nm	0.38	7.97	nes	8.41	7.74
	0.67	7.69	nes	8.15	7.61
	1.08	7.49	nes	7.83	7.48
	1.67	7.44	nes	7.53	7.36
	2.5	7.44	nes	7.45	7.24

nes: not enough sample for diffusion experiment.

Table A3. Diffusion Coefficients of AVR-9 and Its Subfractions

		$\overline{D} \times 10^6$ (cm^2/s)			
	t (h)	Fraction	Saturates	Aromatics	Resins
15 nm	1. 5	5.40	nes	5.50	5.10
	3	5.20	nes	5.24	4.73
	5.5	4.90	nes	5.10	4.56
	10	4.58	nes	5.00	4.37
	17.5	4.43	nes	4.89	4.26
50 nm	0.38	6.44	nes	6.79	6.08
	0.67	6.36	nes	6.52	5.91
	1.08	6.29	nes	6.40	5.84
	1.75	6.05	nes	6.30	5.76
	2.83	5.87	nes	6.27	5.58
80 nm	0.38	6.95	nes	6.91	6.71
	0.67	6.77	nes	6.77	6.52
	1.08	6.62	nes	6.69	6.35
	1.75	6.42	nes	6.58	5.20
	2.83	6.27	nes	6.38	6.14
1000 nm	0.38	7.13	nes	7.21	7.14
	0.67	7.05	nes	7.00	6.98
	1.08	6.81	nes	6.73	6.76
	1.75	6.63	nes	6.56	6.47
	2.83	6.39	nes	6.43	6.29

nes: not enough sample for diffusion experiment.

Table A4. Diffusion Coefficients of AVR-12 and Its Subfractions

		$\overline{D} \times 10^6$ (cm^2/s)			
	t (h)	Fraction	Saturates	Aromatics	Resins
15 nm	1. 5	3.58	nes	3.70	3.26
	3	3.36	nes	3.39	3.11
	5.5	3.09	nes	3.26	3.03
	10	2.91	nes	2.88	2.80
	19	2.83	nes	2.64	2.38
50 nm	0.58	5.09	nes	5.19	4.55
	1.17	4.83	nes	5.01	4.42
	1.92	4.64	nes	4.90	4.30
	2.92	4.51	nes	4.75	4.17
	4.25	4.45	nes	4.58	4.09
80 nm	0.58	5.34	nes	5.69	5.30
	1.17	5.15	nes	5.42	5.17
	1.92	5.03	nes	5.25	5.07
	2.92	4.99	nes	5.05	4.92
	4.25	4.87	nes	4.79	4.79
1000 nm	0.58	5.57	nes	5.83	5.51
	1.29	5.31	nes	5.51	5.23
	2.13	5.08	nes	5.22	5.08
	3	5.04	nes	5.13	4.93
	4.25	5.00	nes	5.04	4.79

nes: not enough sample for diffusion experiment.

Manuscript received Mar. 8, 2012, and revision received Jun. 8, 2012.